

Improved 1.5 T Magnetic Resonance Spectroscopy in the Human Calf with a Spatially Selective Radio Frequency Surface Coil

M. Alfonsetti¹, C. Testa², S. Iotti^{2,3}, E. Malucelli², V. Clementi², B. Barbiroli², G. Placidi¹
A. Sotgiu¹ and M. Alecci^{1,*}

¹Dipartimento di Scienze della Salute, Università dell'Aquila, Via Vetoio, 67100, L'Aquila, Italy

²Dipartimento di Medicina Interna, dell'Invecchiamento e Malattie Nefrologiche, Università di Bologna, Via Massarenti 9, Bologna, Italy

³National Institute of Biostructures and Biosystems, Rome, Italy

Abstract: We describe the use of a transverse field RF surface coil that improves 1.5 T proton MR spectroscopy in the human calf. A 2-element figure-of-eight (FO8) transverse field RF surface coil (diameter $2R=10$ cm; separation between the two linear current elements $2s=1$ cm) and a circular loop (CL) coil of equal diameter were built and tested with proton PRESS spectra at 1.5 T. The ¹H PRESS spectra obtained in the resting calf muscle of healthy volunteers showed that the FO8 coil allows a higher PRESS SNR (up to a factor 4.5) within a region of about 20 mm centred at about 12 mm from the coil plane, as compared to a standard CL coil. We found also a faster PRESS SNR decrease in the muscle tissue for anterior/posterior distance >20 mm using the FO8 coil. The measured PRESS SNR in the fat tissues of the calf showed a signal mostly localised within 10 mm from the coils surface and with an improved SNR (up to 5.5 times) observed in the presence of the FO8 coil as compared to the CL coil of equal diameter. The FO8 coil design can be advantageous for MRS applications, since it allows higher SNR from a small VOI positioned centrally within a relatively narrow region at a given depth in the human calf. The reported spatial SNR features of the FO8 coil design should also be useful for ¹H and ³¹P MRS metabolites quantification in the human brain.

Keywords: RF surface coil, B₁ field, PRESS spectroscopy, proton, human calf.

INTRODUCTION

Magnetic Resonance Spectroscopy (MRS) is a well-established tool for the non-invasive investigation of metabolites in the human brain and in the skeletal muscles under various physiological and pathological conditions [1, 2]. MRS studies in humans performed with Radio Frequency (RF) surface coils are usually conducted by a standard circular or rectangular loop of conducting material [3]. This RF coil design produces in the central region of interest (ROI) an RF B₁ field directed perpendicularly to the coil plane (*axial field RF surface coils*). The maximum amplitude of the B₁ field is found at the centre of the coil plane and it decreases as the distance from the coil axis increases. The transmit/receive and/or receive-only axial RF field surface coil is especially suitable for horizontal field MR systems, and in the past two decades it has been successfully used for a number of *in vivo* MRS studies [1-8]. Depending on the specific clinical application the diameter of the circular loop RF coil must be properly selected to allow a full exposure of the tissue/organ under study.

Novel RF surface coil designs comprising one linear current element [9, 10], two crossing linear current elements (butterfly coil) [11], or two parallel linear current elements (figure-of-eight coil, F08) [12-16] positioned in the central

region of the coil were developed to overcome sensitivity and/or spatial selectivity limitations in a given ROI. These geometries are called *transverse field RF surface coils*, because the current flowing in the linear elements produce a B₁ field that, in the central region of the RF coil is, substantially, a transverse RF field (i.e. parallel to the coil plane). In particular, it was shown that specially designed 2-element FO8 coils are suitable for solving the problem of signal loss due to the orientation of the RF surface coil within the scanner [16]. Interestingly, it was also found that for particular geometrical conditions, along the coil axis the FO8 exhibits a pronounced B₁ spatial selectivity, with higher B₁ field amplitude occurring at some distance from the coil plane [14, 15]. A theoretical analysis of transverse field RF surface coils, comprising four centrally positioned linear elements, suitable for 0.35 T vertical magnetic fields MR Imaging (MRI) was described [17]. Recently, a detailed theoretical and experimental analysis of 1.5 T transverse fields RF surface coils comprising 2, 4 or 6 centrally positioned linear elements was reported [18]. It was shown that a careful selection of the elements geometrical disposition allows optimisation of the B₁ field homogeneity in planes parallel to the coil. In a recent work [19], the design of circular loops and butterfly coils giving the optimal intrinsic signal-to-noise ratio (SNR) was investigated. It was shown that, although for the circular loop there is an analytical equation giving the optimal diameter, unfortunately there is no design rule for the butterfly or FO8 coils. A numerical optimisation method, suitable for 3 T butterfly coils of diameter comprised from 4 to 10 cm and loaded with tissue models, was described [19].

*Address correspondence to this author at the Dipartimento di Scienze della Salute, Università dell'Aquila, Via Vetoio, 67100 L'Aquila, Italy;
Tel: +39-0862-433487; Fax: +39-0862-433785;
E-mail: marcello.alecci@univaq.it

Proton MRS studies in the calf of adult volunteers are often performed with a circular or rectangular RF surface coil of about 8-12 cm in size, to be able to cover the full depth of the calf muscles [3-8]. However, the standard RF coil presents a RF B_1 field distribution with a maximum at the coil plane and a progressive decrease along the coil axis. This spatial feature of the RF B_1 field can be deleterious in terms of SNR and selectivity when the tissue of interest has a restricted thickness and is localised at a specific distance from the coil plane.

Transverse field RF surface coils are characterised by a RF field distribution with a sharp B_1 peak located at some distance along the coil axis [14, 15]. This feature makes the use of transverse field RF coils of potential benefit for MRS applications requiring spatial selectivity from a specific ROI. The SNR advantage of the transverse field coil for ^1H MRS was demonstrated with phantoms [20]. Recently, in a preliminary study, we reported the feasibility of the transverse field RF coils for ^1H MRS in the human calf [21].

In the past years, *in vivo* metabolite measurement was performed by means of phased-array of receive-only RF coils [22-25]. The phased-array is composed by a number of axial and/or transverse field RF surface coil elements, disposed with a suitable geometry and operated with electronic means to isolate each coil from the others. More recently, array of RF coils with up to 12 elements have been developed for parallel imaging MRS [26, 27], allowing applications that require high temporal resolution to monitor dynamic systems and/or to reduce the effects of tissue movement.

The aim of the present study was to show that the features of the FO8 coil offers advantages for those *in vivo* MRS applications, where the spatial selectivity and enhancement of the signal from a specific anatomical region of

the sample located at some depth from the surface is preferable. We have numerically investigated the dependence of the RF spatial B_1 selectivity along the coil z-axis of transverse field and standard circular loop RF coils of various diameters. To test the *in vivo* MRS efficacy of the transverse coil design, we have measured the SNR along the coil z-axis by means of 1.5 T ^1H PRESS spectra acquired in the resting calf of adult healthy volunteers. The results reported here should be a useful starting point for the future clinical MRS applications with single transmit/receive RF coils, and also for the design of MRS array comprising a number of transverse field RF coil geometries.

METHODS AND RESULTS

RF Coils Simulation

To compare the RF spatial distributions of a transverse field coil tuned at 64 MHz (proton, 1.5 T) made by two current elements, having the current path connected accordingly to the FO8 geometry, and standard circular loop (CL) coils we used a quasi-static numerical integration of the Biot-Savart law to model the three-dimensional RF B_1 field distributions. Accordingly with previous theoretical and experimental data [15, 16], the FO8 coil diameter ($2R=10$ cm) and the separation between the two linear current elements ($2s=1$ cm) were chosen such that to allow MRS data acquisition in the human calf of adult volunteers. To compare the RF field distributions along the coil z-axis, a FO8 coil of 10 cm in diameter ($2s=1$ cm) and a number of CL coils of diameter equal to 2.5, 3.8, 5.0, 7.5, 10.0 cm were also simulated.

Fig. (1) shows the simulated B_1 amplitude per-unit-current plotted along the coil z-axis. For all the simulations, the B_1 amplitude was normalised to the value of the smaller size ($2R=2.5$ cm) CL at $z=0$ mm. As expected, the small size CL

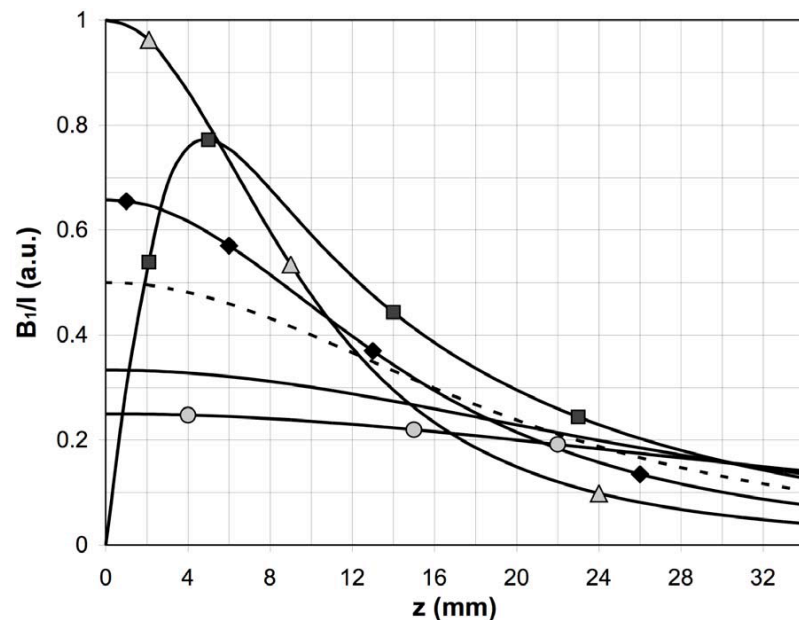


Fig. (1). Normalized B_1 amplitude per-unit-current plotted along the coils z-axis obtained by Biot-Savart simulation. The CL coil has a diameter $2R$ of: 2.5 cm (triangles), 3.8 cm (diamonds), 5.0 cm (dashed line), 7.5 cm (continuous line) and 10.0 cm (circles). The circular figure-of-eight (FO8) RF surface coil (squares) has a diameter $2R=10$ cm and element separation $2s=1$ cm. For all the simulations, the B_1 amplitude was normalised to the value of the smaller size CL at $z=0$ mm.

coil presents the higher B_1 field amplitude within a relatively narrow region close to the surface and a rapid decrease at deeper positions. Moreover, because of the small coil diameter, the region of B_1 sensitivity will be effective only in a very small area of the calf with size similar to the diameter. With such small size coil, to fully cover the calf muscles area a repeated repositioning of the small size coil would be necessary, with the introduction of spatial uncertainty and an increase of the total acquisition time. Alternatively, the use of a phased-array coil design made by a number of overlapping CL coils each connected to a pre-amplifier of suitable impedance would be required, making the hardware complex, expensive, and not readily available. As shown in Fig. (1), increasing the CL diameter ($2R > 2.5$ cm) increases the observable depth, but the normalized peak B_1 field at $z=0$ mm decreases rapidly to about 0.5 ($2R=5$ cm) or about 0.25 ($2R=10$ cm) times the value obtained with the small size CL coil.

On the contrary, as shown in Fig. (1), the FO8 coil of diameter 10 cm exhibits a relatively sharp B_1 peak with normalised B_1 amplitude of about 0.8 with respect to the small size CL. The important features are that the B_1 peak is located at a specific depth ($z=5$ mm) from the coil plane and its peak value is significantly larger as compared to the medium/large size ($2R > 2.5$ cm) CL coils. Because of the symmetry of the two-elements FO8 coil, the peak B_1 field amplitude is centrally located in correspondence of a narrow strip (width about 25 mm, length about 80 mm) aligned with the linear current elements, with the maximum field positioned at some depth from the coil plane. We have previously shown that the width of this strip can be adjusted by a proper selection of the number and separation of the current

elements [18]. Moreover, the position of the peak B_1 field along the z -axis can be adjusted, within a limited range, by the selection of the current elements separation [15]. The above features of the FO8 coil make its use of interest for MRS application in the human skeletal muscles, where a combination of large ROI, good SNR and spatial selectivity at some depth from the coil surface is preferable in some specific studies of muscle metabolism [4-9].

Fig. (2) shows the prototype of FO8 RF surface coil ($2R=10$ cm, two linear current elements, elements separation $2s=1$ cm). For comparison purpose, a standard CL RF coil (not shown) of diameter $2R=10$ cm was used [16]. These coils were tuned at 63.87 MHz and MRI/MRS data were acquired using a 1.5 T GE SIGNA LX 9.1 scanner. This size of the FO8 and CL coils was chosen to allow a large area and depth of the muscle to be covered. As shown in Fig. (1), a small size CL coil ($2R=2.5$ cm) would give maximum B_1 sensitivity at the tissue surface, at the cost of a small area covered and significant signal loss from deeper tissues. The full details of the FO8 and CL coils construction have been reported elsewhere [16].

The B_1 modelling of the CL and FO8 coils reported in Fig. (1) does not take into account the noise contribution detected by each coil. However, previous experimental data obtained at 63.87 MHz have shown that the noise detected by CL and FO8 coils of the same diameter is practically the same [16]. These data justify the use of the Biot-Savart modelling as a useful tool in the design of FO8 and CL coils for MRS applications in the human calf muscles. It is worth to point out that the CL coil presents a higher sensitivity, with respect to the FO8 of the same diameter, when considering the whole volume covered by the coil. However, as it will be

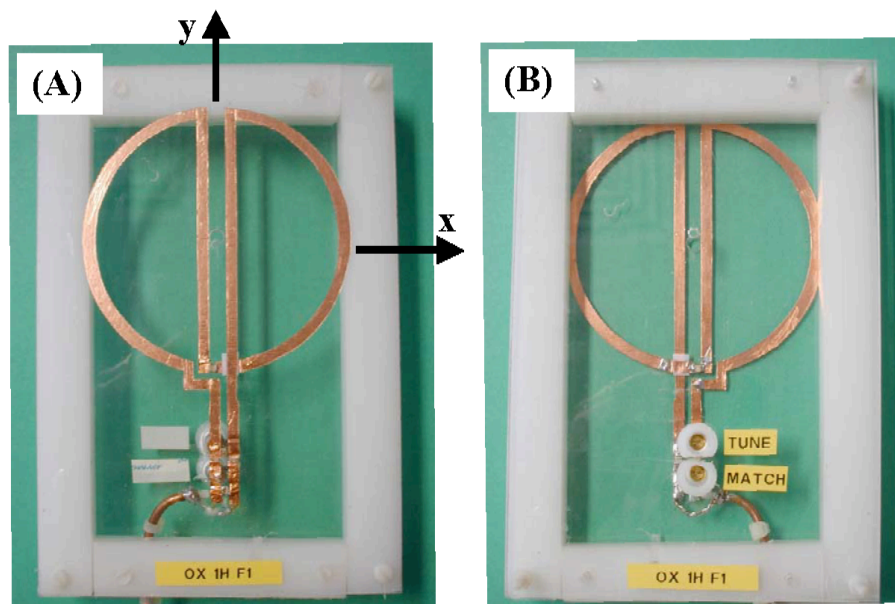


Fig. (2). Circular figure-of-eight (FO8) RF surface coil ($2R=10$ cm, $2s=1$ cm) prototype used for MRS at 1.5 T as seen from the sample side (A) and the service side (B). The y -axis was directed along the B_0 field. The RF coil was constructed on a Plexiglas substrate (thickness 2 mm) using adhesive copper strips of 4 mm width and 100 μ m thickness. A series design was used to connect electrically the left-right loops of the FO8 coil, thus ensuring that the current flowing through the two linear current elements are equal. This series configuration produces negligible phase errors at the operating frequency of 63.87 MHz. Tuning of the RF coil when empty was achieved with a non-magnetic chip capacitor (68 pF) and a non-magnetic trimmer capacitor (1-16 pF) connected in parallel with the inductive current path. A balanced circuit was used for matching the RF coil (two series chip capacitors of 68 pF and a parallel chip capacitor of 470 pF).

shown in the following, when considering a small ROI positioned at some depth from the surface, then the FO8 coil presents a higher sensitivity and a better spatial selectivity that is advantageous for MRS experiments in the human calf muscles.

In Vivo MRS Experiments

To test and characterise the *in vivo* performances obtainable with the FO8 and CL coils, ¹H SPGR scout images and immediately afterwards MRS PRESS spectra were acquired in the presence of the resting calf of two healthy volunteers (average body weight 70 kg; two repeated measurements). Informed consent was obtained from the volunteers, and the local ethics committee approved the project.

In the present study, the FO8 coil was carefully positioned within the scanner with the linear current elements aligned along the direction of the main field B_0 (y-axis in Fig. (2)). For each study, the FO8 and CL coils in turn were used in transmit/receive mode for ¹H localisation, magnetic field shimming, and PRESS spectroscopy on the same VOI positioned at a variable depth from the coil surface. The tuning and matching conditions of the FO8 and CL coils were practically identical. The measured reflection coefficient S_{11} (at the resonance frequency of 63.87 MHz) was better than -25 dB. The measured quality factor Q (ratio between the resonant frequency and the frequency bandwidth at -3 dB) values of the FO8 and CL coils when empty were, respectively, 160 and 195. In the presence of the calf of the volunteers the Q values of the FO8 and CL coils decreased, respectively, to 12 and 14. These loaded Q values are similar to that previously reported by other groups for comparable size RF coils [19]. From repeated measurements, we estimated a small positioning error of the VOI, with respect to the plane of the FO8 and CL coils, equal to about 3 mm in the presence of the calf of the volunteers. It is worth to point out that, since the FO8 RF coil was used in transmit/receive mode and with the current geometrical disposition, the MRI/MRS signal amplitude is dependent from the effective RF field amplitude given by $B_{\text{leff}} = \sqrt{B_{1x}^2 + B_{1z}^2}$, where B_{1x} and B_{1z} are the intrinsic field components of the coil as referred to the geometry of Fig. (2), and the main magnetic field B_0 is assumed to be directed along the y-axis.

First, we acquired scout coronal SPGR images (TE=7 ms; TR=50 ms; flip angle=10°; slice thickness=4 mm; slice spacing=0 mm; FOV=24 cm x 24 cm; NEX=1) for accurate positioning of the voxel along the Anterior/Posterior (A/P) direction (A/P axis is along the z-axis of the RF coil). Given the coil and subject geometry, the first useful SPGR image (slice 1) was positioned at about A/P=2 mm, where the coil plane was taken as A/P=0 mm. From the scout SPGR images of Fig. (3), we note small anatomical differences in the corresponding slices, due to the subsequent positioning of the calf on the FO8 and CL coils.

In accordance with the simulations of Fig. (1), the SNR improvement of the FO8 coil along the A/P direction, as compared to the CL coil, is to be expected only in a relatively small VOI centrally positioned with respect to the linear current elements and within a given depth from the

coil surface. On the contrary, if we consider the whole volume covered by the FO8 or CL coils, we expect the CL coil to perform better in terms of SNR. Moreover, the FO8 coil should give a more pronounced spatial selectivity along the A/P direction. This behaviour of the SNR along the A/P direction can be explained by the fact that the FO8 coil presents, for each centrally positioned linear current element, a return current element of opposite direction positioned at some distance, giving rise to SNR subtraction within the whole volume covered by the coil. This is not the case for the CL coil. However, along the central z-axis (A/P direction) of the FO8 coil the composition of the B_1 field given by the two linear current elements produces the spatially selective SNR pattern shown in Fig. (1), giving rise to an increase of the measured SNR within a relatively small ROI positioned at some distance from the coil surface.

The *in vivo* images of Fig. (3) were used to compare the dependence of the ¹H signal amplitude along the A/P direction for the FO8 and CL coils. To this purpose, first we calculated the SNR of a small ROI covering 0.5*0.5 cm² (8*8 pixels) centrally positioned and then we calculated the SNR of the whole calf covering a ROI of 10*10 cm² (160*160 pixels). The SNR of the selected ROI was calculated as the average signal in the central ROI divided by the standard deviation of the noise calculated in a peripheral ROI (20*20 pixels) external to the muscle. The measured SNR for the small and large ROI are reported, respectively, in Figs. (4A, B). From the data of Fig. (4A) it can be seen that the FO8 coil shows an increased SNR (up to a factor 2) in the small ROI within the slices 4 to 8, as compared to the CL coil. Moreover, for deeper slices (>slice 8) it can be seen that the FO8 coil shows a more pronounced spatial selectivity along the A/P direction. When considering the SNR in a ROI covering the whole calf muscles, see Fig. (4B), it can be seen that the CL coil gives a larger SNR for slices positioned at A/P >4. These MRI results confirm that the SNR advantage of the FO8 coil is to be expected in a small central ROI positioned along the coil axis within the first 2.4 cm from the sample surface. For larger depth and/or considering a large ROI the CL coil gives a better SNR.

To characterize and quantify the dependence of the ¹H MRS amplitude along the A/P direction, we acquired PRESS spectra (TE=26 ms; TR=1500 ms; FOV=16 cm; number of repetition=8) in the presence of the human calf from a voxel positioned at the centre of each SPGR coronal slice, both with the FO8 and CL coils, (see Fig. 5). For sensitivity comparison purposes, in all the PRESS measurements the RF power transmit gain (TG) was maintained at the same minimum value (TG=0 dB) allowed by the scanner. In the current experimental setup the voxel size was selected equal to 8x8x4 mm³, which is smaller than the linear current separation of the FO8 coil (2s=10 mm). No water suppression pulse sequence was employed in the current experimental set-up. Fig. (5) shows typical *in vivo* ¹H PRESS spectra obtained along the A/P direction (slices 1 to 9) with the FO8 coil (Fig. 5A) and the CL coil (Fig. 5B). For easy of visualization the PRESS amplitude was normalised to the maximum value measured with the FO8 coil. The PRESS spectra were analysed using Amares, a tool of the jMRUI software package (Magnetic Resonance User Interface, www.mruui.uab.es/mruui) [28]. For each A/P position, we found that the

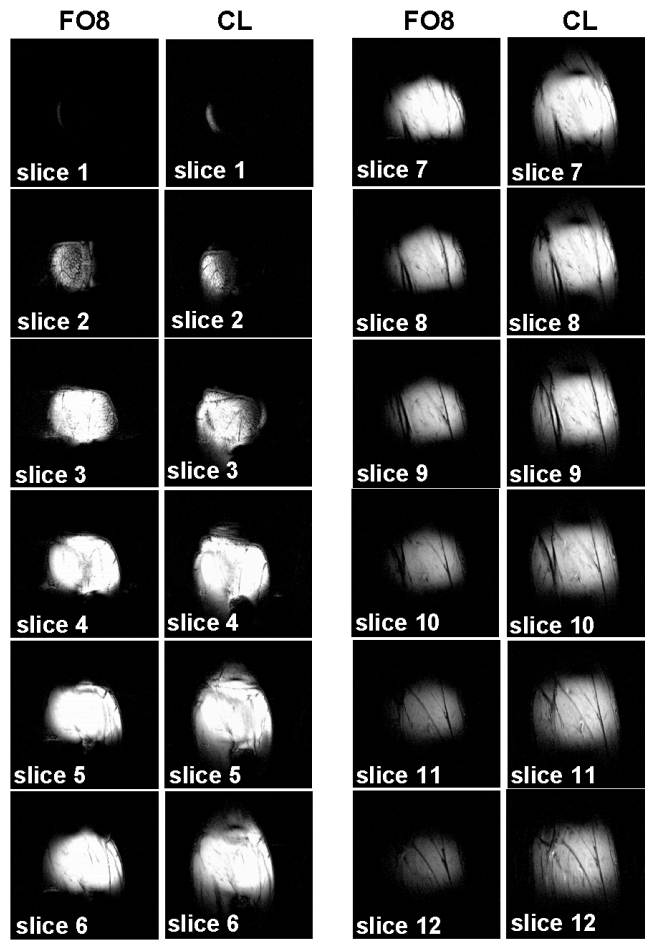


Fig. (3). Typical SPGR coronal images obtained in the resting calf of a volunteer using the FO8 (left) and CL (right) coils. The RF coil plane is positioned at A/P=0 mm and the slice thickness is 4 mm. The slice number equal to 1 is at about 2 mm from the coil plane. The grey scale setting is the same for the images obtained with the FO8 (2R=10 cm, 2s=1 cm) and CL (2R=10 cm) coils.

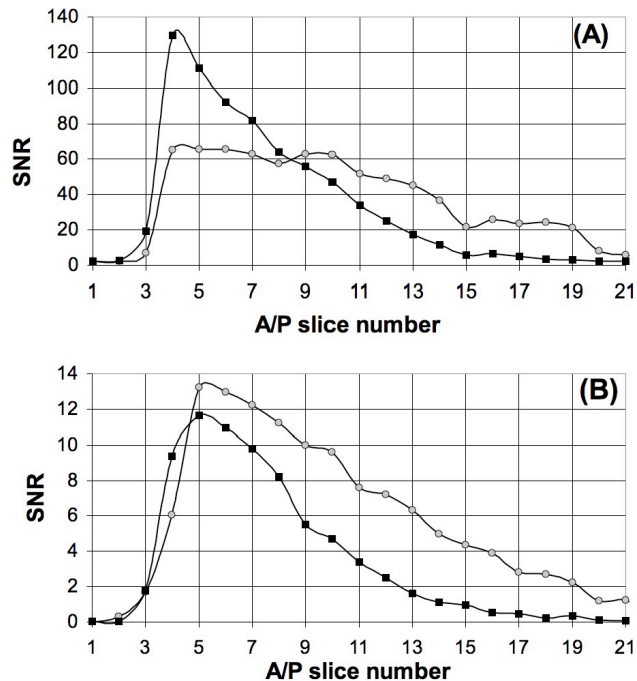


Fig. (4). Measured ¹H SNR along the A/P direction for the FO8 (squares) and CL (circles) coils obtained from the coronal images of Fig. (3) by selecting: (A) a small ROI of 0.5*0.5 cm² centrally positioned within the calf; and (B) a large ROI of 10*10 cm² covering the whole calf.

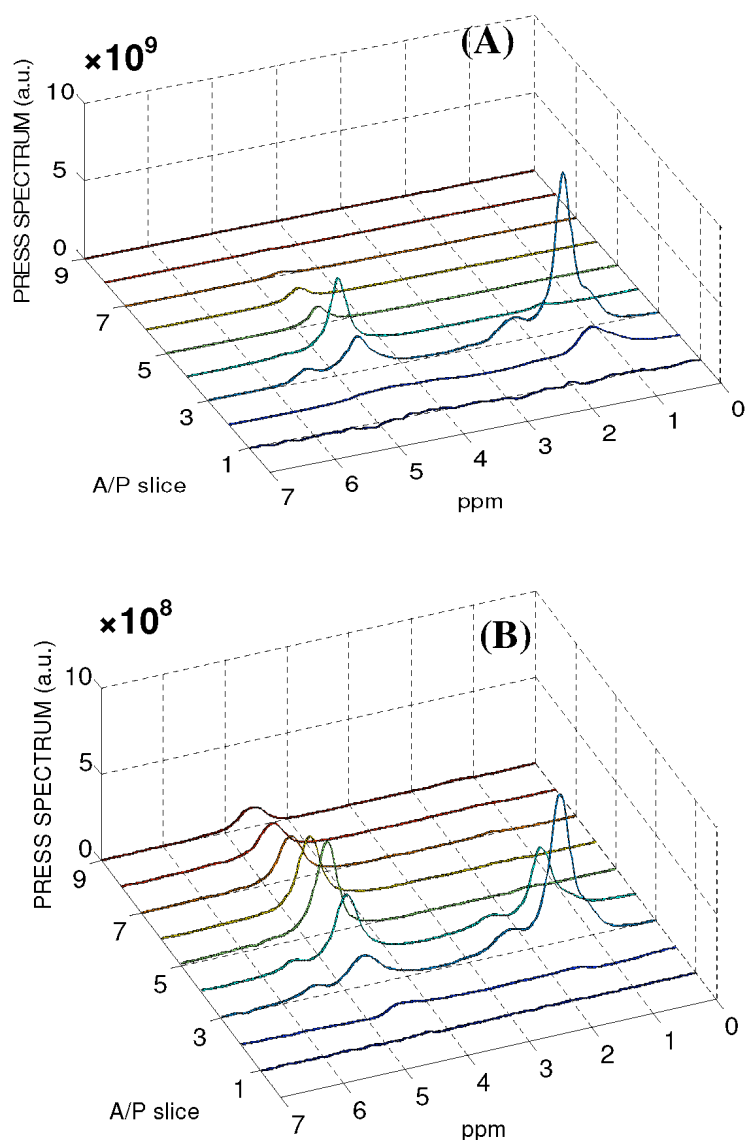


Fig. (5). Typical proton PRESS spectra (voxel size $8 \times 8 \times 4 \text{ mm}^3$; TE=26 ms; TR=1500 ms; number of repetitions=8) measured along the A/P direction in the resting calf of a volunteer using the FO8 (A) and CL (B) RF coils. The position A/P=0 corresponds to the RF coil plane. No water suppression was employed to acquire the PRESS data and the shim setting was the same for the two data sets.

experimental ^1H PRESS spectra showed the presence of white noise with practically the same standard deviation for the FO8 and CL coils.

Fig. (6) shows typical *in vivo* ^1H PRESS spectra obtained along the A/P direction with the FO8 and CL coils at slice=3, this slice corresponding to the position of maximum lipids signal. From the Amares analysis of the *in vivo* spectra we identified a number of peaks, with the resonances specifically assigned in (Table 1), and corresponding to: methyl- of intracellular lipids (IMCL) at 0.9 ppm; methyl- of extracellular lipids (EMCL) at 1.1 ppm; methylene- of intracellular lipids (IMCL) at 1.3 ppm; methylene- of extracellular lipids (EMCL) at 1.5 ppm; α and β methylene- of lipids at 2.3-2.4 ppm; water at 4.7 ppm; and polyunsaturated olefinic fats at 5.5 ppm. These results are in good agreement with previous localized ^1H MRS studies [29-32].

To obtain a quantitative sensitivity comparison of the FO8 and CL RF coils, the area of the ^1H PRESS water peak

(4.7 ppm) component was quantified with the jMRUI software and the SNR for each A/P position was calculated as the area under the peak divided by the noise standard deviation taken away from the peaks. The measured maximum SNR of the water peak, obtained at slice=4, was about 550 and 120 for the FO8 and CL coils, respectively. As shown in (Table 1) the lipid peak components obtained at slice=3 with the FO8 coil showed always a larger SNR in comparison with the CL coil.

Fig. (7) shows the typical spatial dependence (A/P direction) of the SNR obtained with a volunteer, and each data point is the average of two independent measurements. As reported in Fig. (7A), the measured SNR in the water muscle tissue component shows that the FO8 coil allows a higher SNR (up to a factor 4.5) within a region of about 20 mm centred at about 12 mm from the coil plane, narrower than that of the CL coil. As shown in Fig. (7A), we found also a faster decrease of the SNR in the muscle tissue for A/P>20

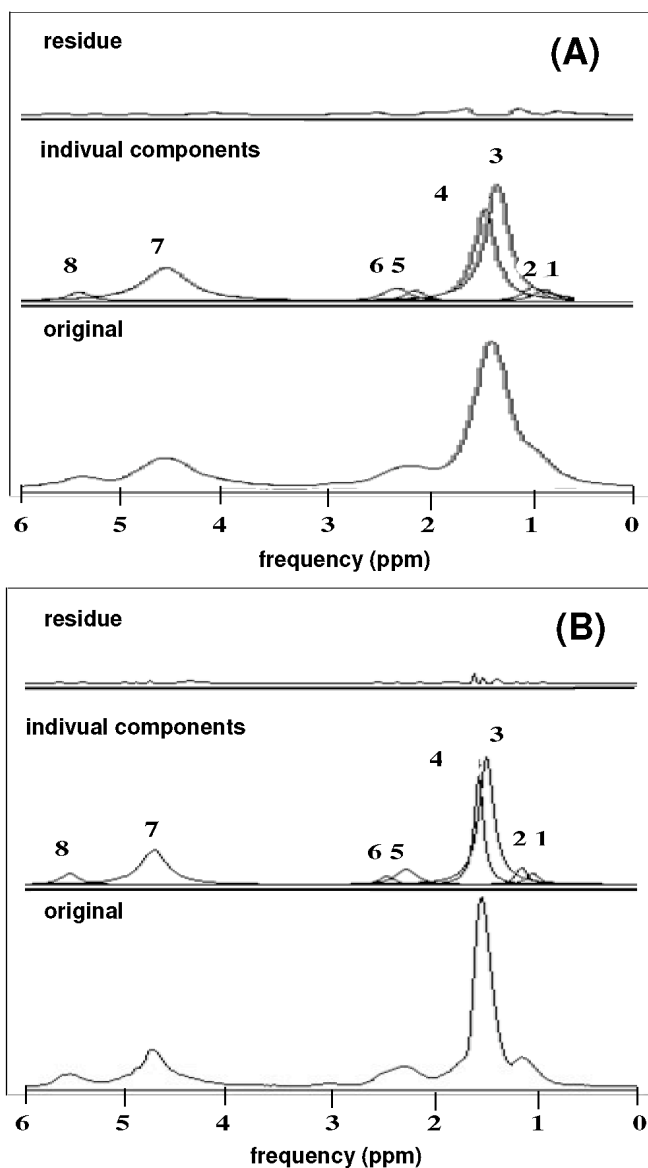


Fig. (6). Analysis of the proton PRESS spectra (voxel size 8x8x4 mm³; TE=26 ms; TR=1500 ms; number of repetitions=8) obtained with the FO8 (A) and CL (B) coils at slice 3, corresponding to the positions of maximum lipids signal.

Table 1. Quantitative Parameters of the JMRUI Analysis of the Proton PRESS Spectra (Voxel Size 8x8x4 mm³; TE=26 ms; TR=1500 ms; Number of Repetitions=8) Obtained with the FO8 and CL Coils at Slice 3

Peak	Frequency (ppm)	Proton Peak Assignment	SNR	
			CL	FO8
1	0.9	IMCL Methyl	10	57
2	1.1	EMCL Methyl	11	76
3	1.3	IMCL Methylene	116	710
4	1.5	EMCL Methylene	92	364
5	2.3	α and β Methylene	9	126
6	2.4	α and β Methylene	14	48
7	4.7	Water	65	352
8	5.5	Polyunsaturated Olefinic Fats	9	77

mm using the FO8 coil, as compared to the CL coil. This spatial selectivity feature of the FO8 coil, as compared to the CL coil, is also shown in the axial fast gradient echo images of Figs. (7C) and (D).

Because of the fat superficial location and the relative sensitivities of the RF coils, the spatial dependence of the measured SNR in the fat tissues are very similar for the FO8 and CL coils, with the signal mostly localised in a narrow region of about 10 mm close to the coil plane, as reported in Fig. (7B). In the fat tissues the measured SNR with the FO8 coil is about 5.5 times that obtained with the CL coil.

CONCLUSIONS

We have described the use of a FO8 transverse field RF surface coil suitable for proton MRS at 1.5 T. *In vivo* MRS studies have shown that along the A/P direction this FO8 coil allows in the human calf tissues for the water peak a higher SNR (up to a factor 4.5) within a narrow (about 20 mm) region centred at a given distance (about 12 mm) from the coil plane, as compared to a standard CL coil of equal diameter. Moreover, the FO8 coil shows a more pronounced signal decrease in the muscle tissues for deeper locations (A/P > 20 mm) tissues, as compared to the CL coil. This behaviour of the PRESS SNR for the muscle tissues along the A/P direction can be explained by the fact that the FO8 coil presents,

for each centrally positioned linear current element, a return current element of opposite direction positioned at some distance, giving rise to SNR subtraction within the whole volume covered by the coil. This is not the case for the CL coil. However, along the central z-axis (A/P direction) of the FO8 coil the superposition of the B_1 field given by the two close linear current elements produces a spatially selective SNR pattern (see Fig. 7), giving rise to an increase of the measured PRESS SNR within a relatively small ROI positioned at some distance from the coil surface. The measured PRESS SNR in the fat tissues of the calf showed a signal mostly localised in a narrow region (about 10 mm) close to the coils plane, and with an improved SNR (up to 5.5 times) observed in the presence of the FO8 coil as compared to the CL coil. The measured SNR spatial distributions obtained with the PRESS data are in good qualitative agreement with our simulated RF distributions (Fig. 1) and also with previous theoretical work [12].

We have shown that this RF FO8 coil can be helpful in improving the SNR of both water and lipids ^1H NMR spectra acquired in the human calf in a relatively narrow region. The above features of the FO8 coil design should also be of benefit in several clinical MRS applications, as for example in ^{31}P MRS metabolic studies of the human calf muscles under force-controlled plantar flexion exercise [5-8], where it is useful to increase SNR in muscles close to the surface (e.g.

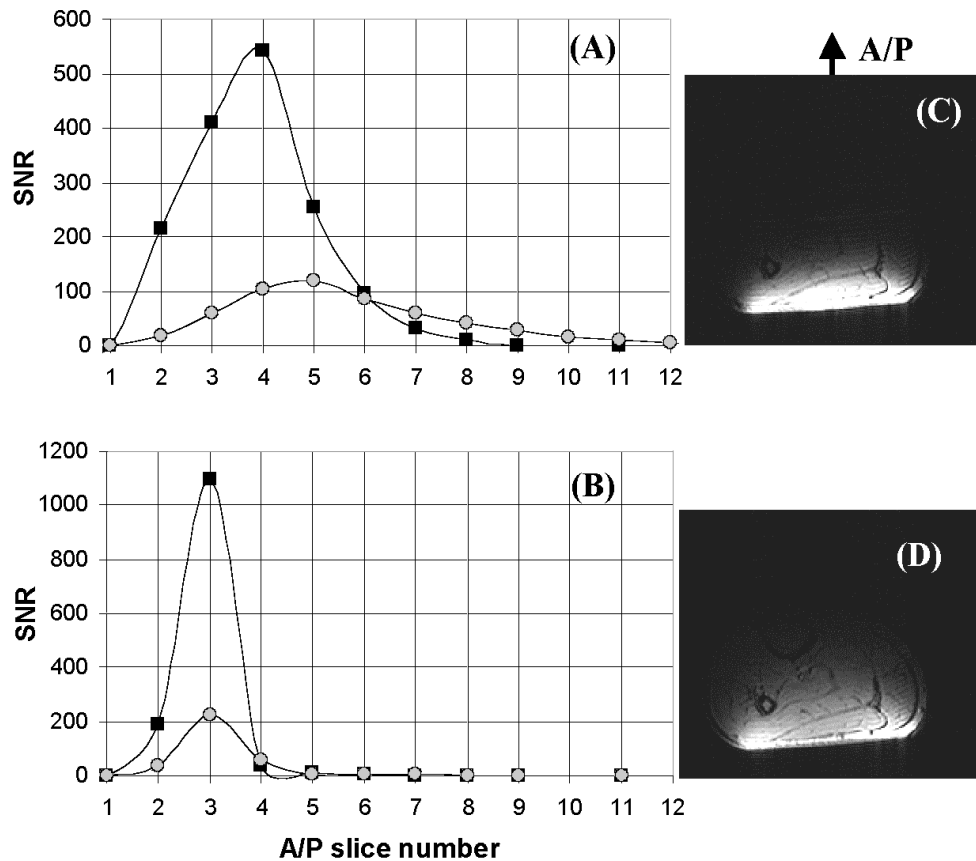


Fig. (7). SNR along the A/P direction obtained from the PRESS spectra using the FO8 (squares) and CL (circles) RF coils and considering the two main spectral components: the water peak at 4.7 ppm (A) and the total fat peaks comprised between 0.9-1.5 ppm (B). The first useful voxel ($8 \times 8 \times 4 \text{ mm}^3$) was at about A/P=4 mm (slice number 2) from the RF coil plane, corresponding to A/P=0 mm. The calf anatomy of the volunteer is shown in the axial fast gradient echo images (TE=2 ms; TR=64 ms; flip angle=30°; slice thickness 5 mm; FOV=15 cm x 15 cm; NEX=1) obtained with the FO8 (C) and CL (D) coils. The grey scale setting is the same for the two images.

gastrocnemius) and to attenuate signal contribution from deeper muscles (e.g. soleus). Also the increased SNR could be useful for improving the quantification of lipids content in muscles [29-32] and the spatial resolution of spectroscopic imaging of the human skin [33, 34]. The reported spatial SNR features of the FO8 coil design should also be useful for ^1H and ^{31}P MRS metabolites quantification in the human brain [1, 2, 35].

ACKNOWLEDGEMENTS

We would like to thank Professor Raffaele Lodi for helpful discussions. We thank Dr. Cristina Santoli and Ms. Carmelita Marinelli for technical assistance.

REFERENCES

- [1] Salibi N, Brown MA. Clinical MR spectroscopy: first principles. New York: Wiley-Liss 1998.
- [2] Tofts PS, Waldman AD. Spectroscopy: ^1H Metabolite concentrations. In: Tofts PS, Ed. Quantitative MRI of the brain. Chap. 9: Chichester: Wiley, 2004; pp. 299-339.
- [3] Ackerman JJH, Grove TH, Wong GG, Gadian DG, Radda GK. Mapping of metabolites in whole animals by ^{31}P NMR using surface coils. *Nature* 1980; 83: 167-70.
- [4] Zaniol P, Serafini M, Ferraresi M, *et al.* Muscle ^{31}P -MR spectroscopy performed routinely in a clinical environment by a whole-body imager/spectrometer. *Phys Med* 1992; 8: 87-91.
- [5] Newcomer BR, Boska MD. T1 measurements of ^{31}P metabolites in resting and exercising human gastrocnemius/soleus muscle at 1.5 Tesla. *Magn Reson Med* 1999; 41: 486-94.
- [6] Iotti S, Frassinetti C, Alderighi L, Sabatini A, Vacca A, Barbiroli B. *In vivo* ^{31}P -MRS assessment of cytosolic $[\text{Mg}^{++}]$ in the human skeletal muscle in different metabolic conditions. *Magn Reson Imag* 2000; 18: 607-14.
- [7] Krssák M, Mlynárik V, Meyerspeer M, Moser E, Roden M. ^1H NMR relaxation times of skeletal muscle metabolites at 3 T. *Magn Reson Mater Phys* 2004; 16: 155-9.
- [8] Meyerspeer M, Krssak M, Kemp GJ, Roden M, Moser E. Dynamic interleaved $^1\text{H}/^{31}\text{P}$ STEAM MRS at 3 Tesla using a pneumatic force-controlled plantar flexion exercise rig. *Magn Reson Mater Phys* 2005; 18: 257-62.
- [9] Boskamp E. Magnetic resonance imaging apparatus comprising a quadrature coil system. U.S. Patent 4,816,765, March 28, 1989.
- [10] Oppelt R, Duerr W, Siebold H. Surface resonator for a magnetic resonance imaging apparatus. U.S. Patent 5,153,517, October 6, 1992.
- [11] Bottomley PA. NMR probe with multiple isolated coplanar surface coils. U.S. Patent 4,973,908, November 27, 1990.
- [12] Boskamp E. Magnetic resonance imaging apparatus with a decoupling detection surface coil. U.S. Patent 4,839,595, June 13, 1989.
- [13] Smith MA, Pye DW. A surface coil design for a vertical field MRI system and its application in imaging the breast. *Magn Reson Imag* 1986; 4: 455-46.
- [14] Seton HC, Hutchinson JMS, Bussel DM. Gradiometer pick-up coil design for a low field SQUID-MRI system. *Magn Reson Mater Phys* 1999; 8: 116-20.
- [15] Alfonsetti M, Placidi G, Sotgiu A, Alecci M. Design of figure-of-eight radio frequency surface coils for MRI at 1.5 T. Proceedings of the 20th Meeting of the ESMRMB; September 18-21; Rotterdam, Holland 2003; p. s224.
- [16] Alfonsetti M, Clementi V, Iotti S, *et al.* Versatile coil design and positioning of transverse-field RF surface coils for clinical 1.5-T MRI applications. *Magn Reson Mater Phys* 2005; 18: 69-75.
- [17] Tang B, Bao S, Zu D, Deng Y, Yongxing JI. Optimization of RF coil for vertical magnetic field MRI. Proceedings of the 7th Meeting of the ISMRM; May 22-28; Philadelphia, USA 1999; p. 2064.
- [18] Alfonsetti M, Mazza T, Alecci M. Optimisation of multi-element transverse field radio frequency surface coils. *Meas Sci Technol* 2006; 16: N53-9.
- [19] Kumar A, Bottomley PA. Optimized quadrature surface coil designs. *Magn Reson Mater Phys* 2008; 21: 41-52.
- [20] Alfonsetti M, Clementi V, Iotti S, *et al.* Improved proton MRS at 1.5 T with a transverse field RF surface coil. Proceedings of the 13th Meeting of the ISMRM; May 7-13; Miami, USA 2005; p. 2503.
- [21] Alfonsetti M, Testa C, Iotti S, *et al.* ^1H MRS in the human calf with a spatially selective RF surface coil. Proceedings of the 15th Meeting of the ISMRM; May 5-9; Toronto, Canada 2008; p. 2600.
- [22] Hardy CJ, Bottomley PA, Rohling KW, Roemer PB. An NMR phased array for human cardiac ^{31}P spectroscopy. *Magn Reson Med* 1992; 28: 54-64.
- [23] Natt O, Bezkorovaynyy V, Michaelis T, Frahm J. Use of phased array coils for a determination of absolute metabolite concentrations. *Magn Reson Med* 2005; 53: 3-8.
- [24] Dong Z, Peterson B. The rapid and automatic combination of proton MRSI data using multi-channel coils without water suppression. *Magn Reson Imaging* 2007; 25: 1148-54.
- [25] Osorio JA, Ozturk-Isik E, Xu D, *et al.* 3D ^1H MRSI of brain tumors at 3.0 Tesla using an eight-channel phased-array head coil. *J Magn Reson Imaging* 2007; 26: 23-30.
- [26] Lin FH, Tsai SY, Otazo R, *et al.* Sensitivity-encoded (SENSE) proton echo-planar spectroscopic imaging (PEPSI) in the human brain. *Magn Reson Med* 2007; 57: 249-57.
- [27] Tsai SY, Otazo R, Posse S, *et al.* Accelerated proton echo planar spectroscopic imaging (PEPSI) using GRAPPA with a 32-channel phased-array coil. *Magn Reson Med* 2008; 59: 989-98.
- [28] Naressi A, Couturier C, Devos JM, *et al.* Java-based graphical user interface for the MRUI quantitation package. *Magn Reson Mater Phys* 2001; 12: 141-52.
- [29] Boesch C, Slotboom J, Hoppeler H, Kreis R. *In vivo* determination of intra-myocellular lipids in human muscle by means of localized ^1H -MR spectroscopy. *Magn Reson Med* 1997; 37: 484-93.
- [30] Steidle G, Machann J, Claussen CD, Schick F. Separation of intra- and extramyocellular lipid signals in proton MR spectra by determination of their magnetic field distribution. *J Magn Reson* 2002; 154: 228-35.
- [31] Newcomer BR, Lawrence JC, Buchthal S, den Hollander JA. High-resolution chemical shift imaging for the assessment of intramuscular lipids. *Magn Reson Med* 2007; 57: 848-58.
- [32] Velan SS, Durst C, Lemieux S, *et al.* Investigation of muscle lipid metabolism by localized one- and two-dimensional MRS techniques using a clinical 3T MRI/MRS scanner. *J Magn Reson Imaging* 2007; 25: 192-9.
- [33] Weis J, Ericsson A, Hemmingsson A. Chemical shift artifact-free microscopy: spectroscopic microimaging of the human skin. *Magn Reson Med* 1999; 41: 904-08.
- [34] Weis J, Ericsson A, Astrom G, Szomolanyi P, Hemmingsson A. High-resolution spectroscopic imaging of the human skin. *Magn Reson Imaging* 2001; 19: 275-8.
- [35] Bonavita S, Di Salle F, Tedeschi G. Proton MRS in neurological disorders. *Eur J Radiol* 1999; 30: 125-31.